11th World Congress on Computational Mechanics (WCCM XI)
5th European Conference on Computational Mechanics (ECCM V)
6th European Conference on Computational Fluid Dynamics (ECFD VI)
E. Oñate, J. Oliver and A. Huerta (Eds)

# NUMERICAL ANALYSIS OF FLOW-INDUCED VIBRATION OF TWO CIRCULAR CYLINDERS IN TANDEM AT LOW REYNOLDS NUMBERS

**PAULO R. F. TEIXEIRA[*] AND ERIC DIDIER[†]**

[*] Universidade Federal do Rio Grande
Avenida Itália km8, Campus Carreiros, Rio Grande, RS, 96201-900, Brazil
e-mail: pauloteixeira@furg.br, www.furg.br

[†] Departamento de Hidráulica e Ambiente
Laboratório Nacional de Engenharia Civil
Av. do Brasil, 101,1700-066, Lisboa, Portugal
email: edidier@lnec.pt, www.lnec.pt

**Key Words:** *Finite Element Method, Flow-induced Vibration, Circular Cylinders, Tandem Arrangement, Wake Interference*

**Abstract.** Uniform flows over circular cylinders in different arrangements appear in many practical situations. Analyses of side-by-side, tandem and staggered arrangements have shown significant differences among flow parameters and the interaction of the flow and the cylinder, by comparison with single cylinder parameters. This paper describes the study of two circular cylinders in tandem arrangement subject to bi-dimensional uniform laminar flows at low Reynolds numbers from 90 to 140. Cases with distance between cylinders equal to 5.25 diameter for both fixed cylinders and for a fixed upstream cylinder and a downstream one elastically mounted in transversal direction are analysed. The numerical model Ifeinco, which is based on the finite element method and uses a partitioned scheme that considers two-way interaction of fluid flow and structure, is employed in the analysis. The fluid flow model uses a semi-implicit two-step Taylor-Galerkin method to discretize the Navier-Stokes equations and the arbitrary Lagrangean-Eulerian formulation to follow the cylinder motion. The analysis of the cylinder movement is carried out by using one DOF dynamic equation for the transverse direction discretized in time by the implicit Newmark method. For both fixed cylinders, differences in terms of lift and drag coefficients and Strouhal number are found by comparison with the ones of the single cylinder. When the downstream cylinder is elastically mounted, a lock-in phenomenon is observed in a range of Reynolds numbers, characterized by the discontinuity of the lift and drag coefficients, vortex vibration and natural frequencies approximation and increase in vibration amplitude.

## 1 INTRODUCTION

The vortex-induced vibration phenomenon can occur as a result of the action of wind on bridges, slender buildings, chimneys and energy transmission cables besides the action of water flow on pipelines and risers. The wake around circular cylinders due to a uniform flow leads to

several complex phenomena. Despite the simplicity of geometry, the flow around cylinders requires deep studies, since it may induce unsteady forces on structures associated with vortex shedding.

This phenomenon, which appears in many practical situations of different bluff body arrangements, has its complexity increased due to the wake interference among circular cylinders. Side-by-side, tandem and staggered arrangements between two equal diameter cylinders are specific cases that are currently used to explain this interference. Analyses of these types of arrangements have shown significant differences among flow parameters and the interaction of the flow and the cylinder, by comparison with single cylinder parameters. Several interference regimes have been classified, according to the Reynolds number and distance between cylinders, based on experimental studies, such as Igarashi's [1], Zdravkovich's [2,3] and Sumner et al.'s [4]. Considering tandem arrangement of circular cylinders [1,5], a critical distance, *Lc*, between both cylinders is identified ($L/D \approx 4$, where $L$ is the center to center distance between cylinders and $D$ is the diameter) in which discontinuity of the flow behavior and vortex shedding occur. For shorter distances ($L < Lc$), the mean drag of the downstream cylinder is small and negative. For longer distances ($L > Lc$), fluctuating lift and drag forces of the downstream cylinder become higher than the upstream ones.

Researchers, such as Zdravkovich [6], Brika and Laneville [7], investigated experimentally the flow induced oscillations of two interfering circular cylinders considering different arrangements and distances between them. The authors observed that the vortex induced oscillations are strongly dependent on the arrangement of cylinders and the gap between cylinders. Assi et al. [8], Okajima et al. [9] and Huera-Huarte and Gharib [10] analyzed experimentally the flow induced oscillations specifically for tandem arrangements.

Other researchers, such as Li et al. [11], Slaouti and Stanby [12], Mittal et al. [13], Meneghini et al. [14], Sharman et al. [15], Carmo [16], Carmo and Meneghini [17], studied several parameters of the flow for different arrangements between cylinders based on numerical simulations. Some numerical analyses (Carmo et al. [18], Mittal and Kumar [19], Papaioannou et al. [20]) have been developed for the study of fluid-structure interaction in tandem arrangements of circular cylinders considering two-dimensional cases at different Reynolds numbers, by using vortex discrete method, finite volume method and spectral element method. Carmo et al. [18] condidered the fixed upstream cylinder and the free downstream one to oscillate in transverse direction subjected to flows at Reynolds numbers equal to 150 (bi-dimensional simulation) and 300 (three-dimensional simulation) and varied the reduced velocity by changing the structural stiffness. They concluded that there are significant changes in the dynamic behavior of the cylinders by comparison with a single cylinder.

This paper describes the study of two circular cylinders in tandem arrangement subject to bi-dimensional uniform laminar flows at low Reynolds numbers (from 90 to 140). Cases with center to center distance between cylinders equal to $5.25D$ for both fixed cylinders and for fixed upstream cylinder and a downstream one elastically mounted in transversal direction are analysed. The numerical model Ifeinco [21] which is based on the finite element method and uses a partitioned scheme that considers two-way interaction of fluid flow and structure is employed for the analysis. The fluid flow model uses a semi-implicit two-step Taylor-Galerkin method to discretize the Navier-Stokes equations and the arbitrary Lagrangean-Eulerian formulation to follow the cylinder motion. The classical Galerkin weighted residual method is applied to the space discretization and a triangular element is employed. The cylinder

movement is carried out by using the one DOF dynamic equation for the transverse direction discretized in time by the implicit Newmark method.

## 2 IFEINCO MODEL

The numerical model Ifeinco is based on a partitioned scheme, in which the fluid flow and the structure are solved in two-way interaction. Essentially, the fluid-structure interaction adopted by the code consists in the following steps: (a) update the variables of the flow from instant $t$ to $t+\Delta t$; (b) impose pressure and viscous stress as a load to the structure; (c) update the variables of the structure from instant $t$ to $t+\Delta t$; (d) impose the body motion to the flow in terms of the updated velocity vector and boundary position.

Basically, updating the variables of the flow consists of following steps [22]:

a) Calculate non-corrected momentum per volume $\tilde{U}_i$ at $t+\Delta t/2$, where the pressure term is at $t$ instant, according to Eq. (1).

$$\tilde{U}_i^{n+1/2} = U_i^n - \frac{\Delta t}{2}\left(\frac{\partial f_{ij}^n}{\partial x_j} - \frac{\partial \tau_{ij}^n}{\partial x_j} + \frac{\partial p^n}{\partial x_i} - w_j^n \frac{\partial U_i^n}{\partial x_i}\right) \tag{1}$$

where $p$ is the pressure, $w_i$ are the velocity components of the reference system, $\tau_{ij}$ is the viscous stress tensor, $U_i = \rho \mathrm{v}_i$, $f_{ij} = \mathrm{v}_j(\rho \mathrm{v}_i) = \mathrm{v}_j U_i$ $(i, j = 1, 2)$, $\rho$ is the specific mass and $\mathrm{v}_i$ are the velocity components.

b) Update the pressure $p$ at $t+\Delta t$, given by the Poisson equation:

$$\frac{1}{c^2}\Delta p = -\Delta t\left[\frac{\partial \tilde{U}_i^{n+1/2}}{\partial x_i} - \frac{\Delta t}{4}\frac{\partial}{\partial x_i}\frac{\partial \Delta p}{\partial x_i}\right] \tag{2}$$

where $\Delta p = p^{n+1} - p^n$ and $i = 1, 2$.

c) Correct the velocity at $t+\Delta t/2$, adding the pressure variation term from $t$ to $t+\Delta t/2$, according to the equation:

$$U_i^{n+1/2} = \tilde{U}_i^{n+1/2} - \frac{\Delta t}{4}\frac{\partial \Delta p}{\partial x_i} \tag{3}$$

d) Calculate the velocity at $t+\Delta t$ using variables updated in the previous steps as follows:

$$U_i^{n+1} = U_i^n - \Delta t\left(\frac{\partial f_{ij}^{n+1/2}}{\partial x_j} - \frac{\partial \tau_{ij}^{n+1/2}}{\partial x_j} + \frac{\partial p^{n+1/2}}{\partial x_i} - w_j^{n+1/2}\frac{\partial U_i^{n+1/2}}{\partial x_i}\right) \tag{4}$$

The classical Galerkin weighted residual method is applied to the space discretization of Eq. (1), (2), (3) and (4), and a triangular element is employed. In the variables at $t+\Delta t/2$ instant, a constant shape function is used, and in the variables at $t$ and $t+\Delta t$, a linear shape function is employed [21].

The Poisson equation, which is a result of spatial discretization of Eq. (2), is solved by employing the conjugate gradient method with a diagonal preconditioning [23]. Spatially discretized Equation (4) is explicitly solved by the iterative process using the lumped matrix

[24]. The scheme is conditionally stable and the local stability condition for element $E$ is given by

$$\Delta t_E \leq \beta h_E / |\mathrm{v}| \tag{5}$$

where $h_E$ is the characteristic size of the element (lowest element edge), $\beta$ is the safety factor (0.25 has been adopted in this study) and $|\mathrm{v}|$ is the fluid velocity.

The mesh velocity transversal component $w_2$ is computed to diminish element distortions, keeping prescribed velocities on moving and stationary boundary surfaces. The mesh movement algorithm adopted in this paper uses a smoothing procedure for the velocities based on these boundary lines. The updating of the mesh velocity at node $i$ of the finite element domain is based on the mesh velocity of the nodes $j$ that belong to the boundary lines [21].

In order to update the rigid body motion of the structure, it is necessary to calculate displacements and rotations of a hypothetical concentrated mass at its gravity center. In this case study, there is only movement in transverse direction (one degree of freedom – DOF) and, consequently, displacement, velocity and acceleration in this direction are the variables to be determined at each time step. To update the variables of the structure, the rigid motion of the cylinder is calculated at each instant, after the variables of the flow (pressure and viscous stress) are known. For this case study, one DOF dynamic equation is considered for the transverse direction, as follows:

$$m\ddot{y} + c\dot{y} + ky = F \tag{8}$$

where $\ddot{y}$, $\dot{y}$ and $y$ are the transverse acceleration, velocity and displacement, respectively; $m$ is the mass; $c$ is the damping coefficient; $k$ is the stiffness; and $F$ is the dynamic force. In Ifeinco code, Eq. (8) is discretized in time by using the implicit Newmark method [25] and the acceleration, the velocity and the displacement in transverse direction are calculated at each time step according to the following algorithm:

a) Initialize ${}^0\ddot{y}$, ${}^0\dot{y}$ e ${}^0y$;

b) Calculate the integration constants;

$$a_0 = \frac{1}{\alpha \Delta t^2};\ a_1 = \frac{\delta}{\alpha \Delta t};\ a_2 = \frac{1}{\alpha \Delta t};\ a_3 = \frac{1}{2\alpha} - 1;\ a_4 = \frac{\delta}{\alpha} - 1;\ a_5 = \frac{\Delta t}{2}\left(\frac{\delta}{\alpha} - 2\right); \tag{9}$$

$$a_6 = \Delta t(1 - \delta);\ a_7 = \delta \Delta t$$

c) Determine the effective stiffness coefficient:

$$k_e = k + a_0\, m + a_1\, c \tag{10}$$

And for each time step:

a) Calculate the effective loads at instant $t+\Delta t$, as follows:

$${}^{t+\Delta t}F_e = {}^{t+\Delta t}F + m\left(a_0\,{}^t y + a_2\,{}^t\dot{y} + a_3\,{}^t\ddot{y}\right) + c\left(a_1\,{}^t y + a_4\,{}^t\dot{y} + a_5\,{}^t\ddot{y}\right) \tag{11}$$

b) Solve the displacements at $t+\Delta t$:

$${}^{t+\Delta t}y = {}^{t+\Delta t}F_e / k_e \tag{12}$$

c) Calculate the accelerations and the velocities at $t+\Delta t$:

$$^{t+\Delta t}\ddot{y} = a_0\left(^{t+\Delta t}y - {}^{t}y\right) - a_2\,{}^{t}\dot{y} - a_3\,{}^{t}\ddot{y} \tag{13}$$

$$^{t+\Delta t}\dot{y} = {}^{t}\dot{y} + a_6\,{}^{t}\ddot{y} + a_7\,{}^{t+\Delta t}\ddot{y} \tag{14}$$

where $\delta$ and $\alpha$ are 0.5 and 0.25, respectively, in this study.

## 3 NUMERICAL SIMULATION

Both cylinders, which are immersed in water, have diameters $D$ = 0.0016 m (Fig. 1). The downstream cylinder (mass $m$ = 0.2979 kg) is elastically mounted in transversal direction. The spring stiffness, $k$, is equal to 579 N/m, resulting in a natural frequency of this system of $f_n$ = 7.016 Hz. The damping coefficient, $c$, is equal to 0.0325 kg/s and the correspondent damper ratio is $\zeta = c / 2m\omega_n = 0.0012$, where $\omega_n$ is the angular frequency. The Reynolds number ($\mathrm{Re} = \rho U\infty D/\mu$, where $\rho$ is the specific mass, $U\infty$ is the free stream velocity, $D$ is the flow cylinder diameter and $\mu$ is the viscosity) ranged between 90 and 140, thus, characterizing a regime in which the vortex street is fully laminar and bi-dimensional. Constant velocity ($U\infty$) is imposed on the inlet boundary whereas, on the lateral boundaries (far from cylinders), a slide condition is imposed; the outlet boundary is free exit, but null pressure is imposed on its center. The main dimensionless parameters that influence the VIV behavior are the reduced velocity ($V_R = U\infty/D\,f_n$), ranging from 5 to 7.8, and the mass ratio ($M = m/\rho D^2$) that is equal to 166 [26].

In this case, in which the center to center distance between cylinders is 5.25$D$, vortices shed off the upstream cylinder and roll up before striking the downstream cylinder; then, they interact strongly with it.

The computational domain consists of a rectangle whose sides have the minimum distance from the cylinders of 100$D$. The cylinder boundary is discretized in 200 segments and the size of the first element around the cylinders is 0.016$D$, totalizing 271683 nodes and 542540 triangular elements [27]. The time step is between $6\text{x}10^{-5}$ s and $8.5\text{x}10^{-5}$ s, according to the Reynolds number.

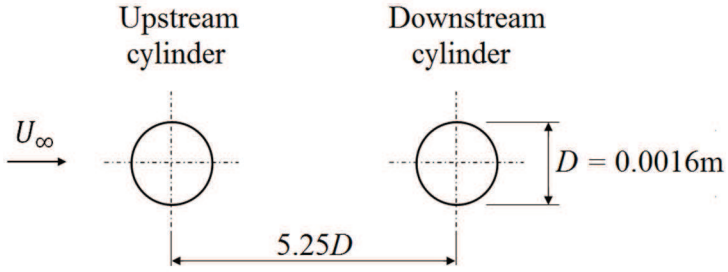


**Figure 1:** Sketch of the case study

### 3.1 Stationary upstream and downstream cylinders

These results are compared with previous ones of a stationary single cylinder obtained by Gonçalves et al. [27]. Results of stationary cylinders in tandem arrangement showed that the Strouhal numbers follow the same trend observed for the single cylinder and are approximately 10% lower than results of a single cylinder along the Reynolds number range (Fig. 2). The shedding frequency happens to be the same for both cylinders for all Reynolds numbers. The root mean square of the lift coefficient ($C_{Lrms}$) for the downstream cylinder is fourfold the one

of the single cylinder, which is similar to the upstream result (Fig. 3). In terms of mean drag coefficients ($C_{Dmean}$), the upstream cylinder presents similar results to the ones of the single cylinder, but the value of the downstream cylinder is approximately half of that of the single one (Fig. 4). These results show that different positions of resonance for tandem arrangement are expected by comparison with the single cylinder case when the downstream cylinder is free, mainly because of differences in Strouhal numbers. Moreover, higher lift coefficients of the downstream cylinder may provide higher vibration amplitudes for tandem arrangement cases by comparison with the single cylinder case, due to the strong interference between both cylinders since the downstream one is placed inside the wake of the upstream one.

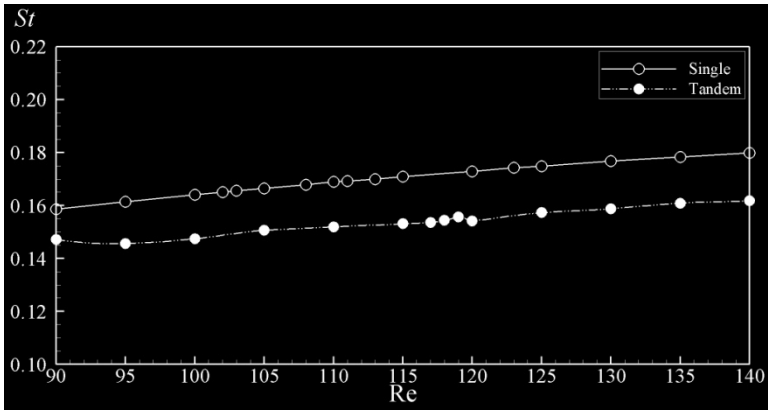


**Figure 2:** Strouhal number versus Reynolds number for stationary cylinder cases

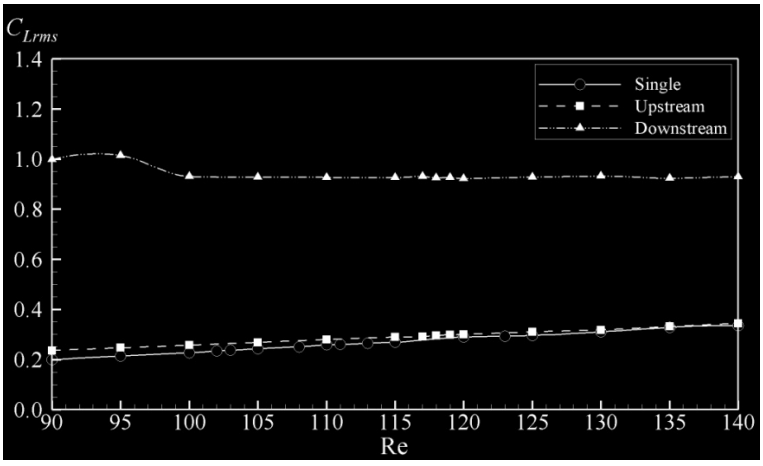


**Figure 3:** Root mean square of lift coefficient versus Reynolds number for stationary cylinders case

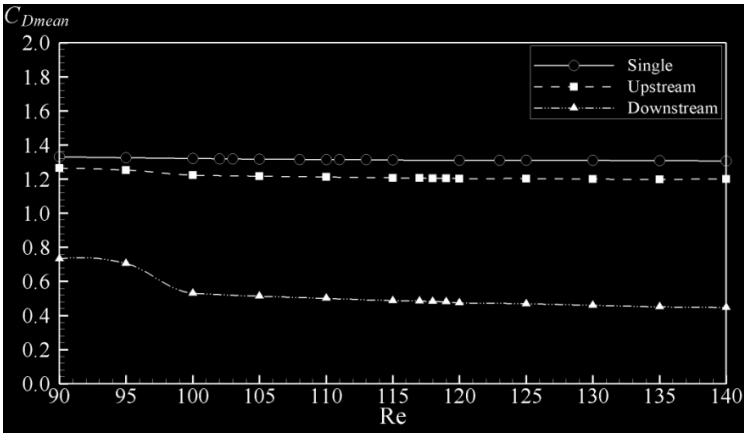


**Figure 4:** Mean drag coefficient versus Reynolds number for stationary cylinder cases

### 3.2 Stationary upstream and oscillating downstream cylinders

When the downstream cylinder is elastically mounted, a significant increase in $C_{Lrms}$ from 1.001 to 1.701 at Reynolds number from 110 ($V_R$ = 6.12) to 119 ($V_R$ = 6.63) and an abrupt decrease in 0.687 at Re = 120 ($V_R$ = 6.68) are observed. This phenomenon is characteristic of the resonance (lock-in) and also occurs in the single cylinder, but with some differences in coefficient magnitude and Reynolds number range, as shown in Fig. 5. The Reynolds number range in which this phenomenon occurs for single cylinder is wider than the range in the tandem arrangement case. Besides, in these regions, the mean drag coefficient for oscillating cylinder gets higher values abruptly, reaching 0.85 for Reynolds number of 117 ($V_R$ = 6.51), as shown in Fig. 6. Similar behavior occurs in the single cylinder case, but with a wider Reynolds number range.

Figure 7 shows the root mean square of lift coefficient and the mean drag coefficient versus Reynolds number for stationary upstream and oscillating downstream cylinders. It may be noticed that while the downstream cylinder experiments high variations of coefficients in the lock-in region, these coefficients decrease smoothly for the upstream cylinder. In this case, flow interference between both cylinders is different from the stationary downstream cylinder due to the motion of the downstream cylinder and changes in wake pattern and pressure field.

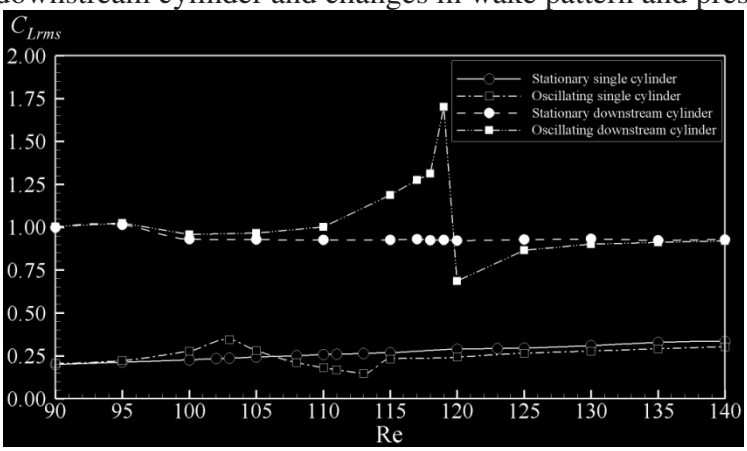


**Figure 5:** Root mean square of the lift coefficient versus Reynolds number for stationary and oscillating downstream cylinders in tandem arrangement and for fixed and oscillating single cylinders

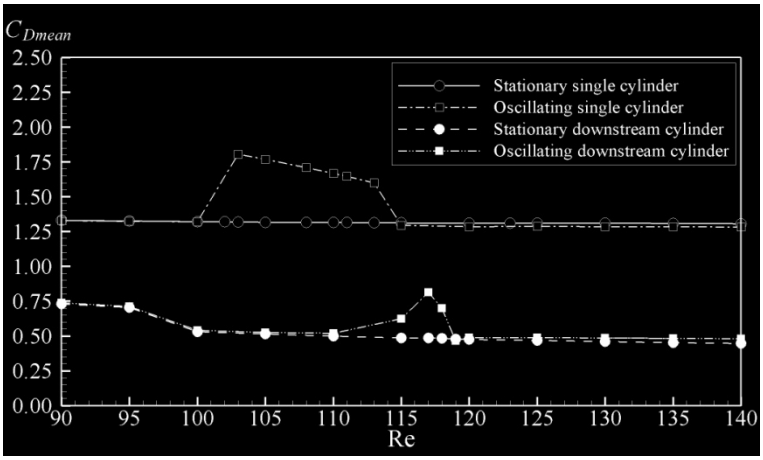


**Figure 6:** Mean drag coefficient versus Reynolds number for stationary and oscillating downstream cylinders in tandem arrangement and for fixed and oscillating single cylinders

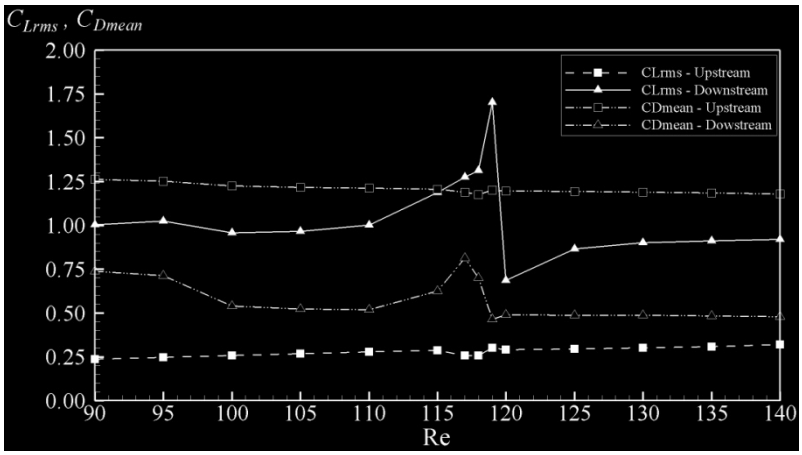


**Figure 7:** Root mean square of lift and mean drag coefficients versus Reynolds number for stationary upstream and oscillating downstream cylinders in tandem arrangement

Figure 8 shows the dimensionless amplitude ($Y/D$) and the vortex induced vibration frequency ($f/f_n$) for downstream cylinder and a comparison with the single one. It can be noticed that the resonance, for the single cylinder, occurred for Reynolds numbers between 102 ($V_R$ = 5.68) and 113 ($V_R$ = 6.29) case in which the vibration amplitude is higher and the vortex frequency is approximately equal to the natural frequency ($f_n$) of the dynamic system. In tandem arrangement with $L/D$ = 5.25, the downstream cylinder experiments the resonance in a shorter Reynolds number range, between 115 ($V_R$ = 6.40) and 120 ($V_R$ = 6.68). Furthermore, the maximum dimensionless amplitude is 0.721 for Re = 118 and this is much higher (more than 70%) than the one for the single cylinder (0.422 for Re = 103). The interference effects on tandem arrangement change the Strouhal number in relation to the single cylinder one and to the mode of interference between both cylinders, since the downstream cylinder is immersed in the periodic wake of the upstream one. This is why there are differences between both lock-in regions.

Figure 9 shows the temporal series of lift coefficient ($C_L$) and dimensionless vibration amplitude ($Y/D$) for Re = 118. Vorticity distributions and streamlines are shown in Fig. 10 where time positions of each picture are indicated in Fig. 9. It may be noticed that the lift coefficient presents higher non linearity by comparison with vibration amplitude which shows harmonic behaviour. The phase angle between them is around 42° in this case. Figure 10 shows that the vortex shedding occurs for both cylinders, as expected for $L/D > 4$, and the wake behind the downstream cylinder is formed by the combination of vortex shed from both cylinders. The maximum vibration amplitude ($Y/D = 0.721$) occurs at instants shown in Fig. 10a and 10b.

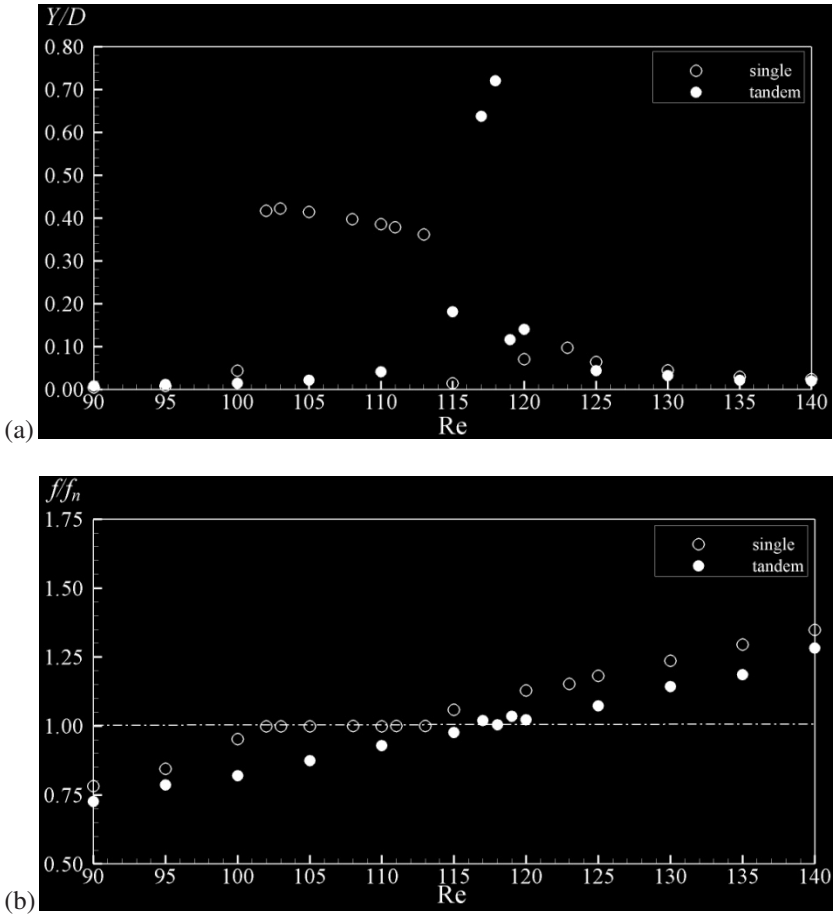


**Figure 8:** Dimensionless vibration amplitude ($Y/D$) (a) and vortex shedding frequency ($f/f_n$) (b) versus Reynolds numbers for single cylinder and cylinders in tandem arrangement

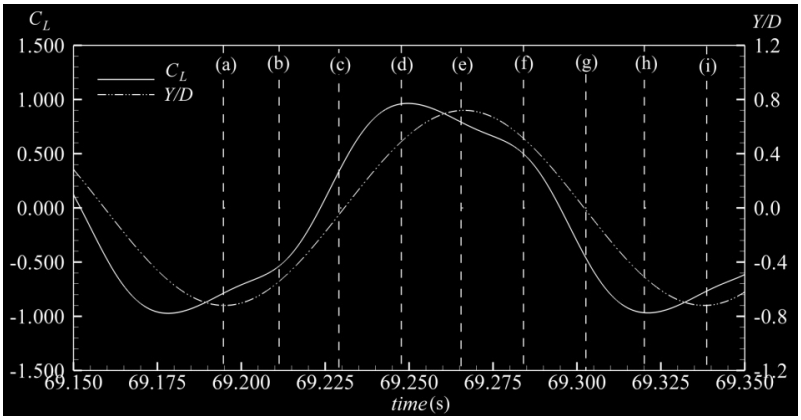


**Figure 9:** Temporal series of lift coefficient ($C_L$) and dimensionless vibration amplitude ($Y/D$) for Re = 118 (letters represent time positions of the vorticity distributions, shown in Fig. 10)

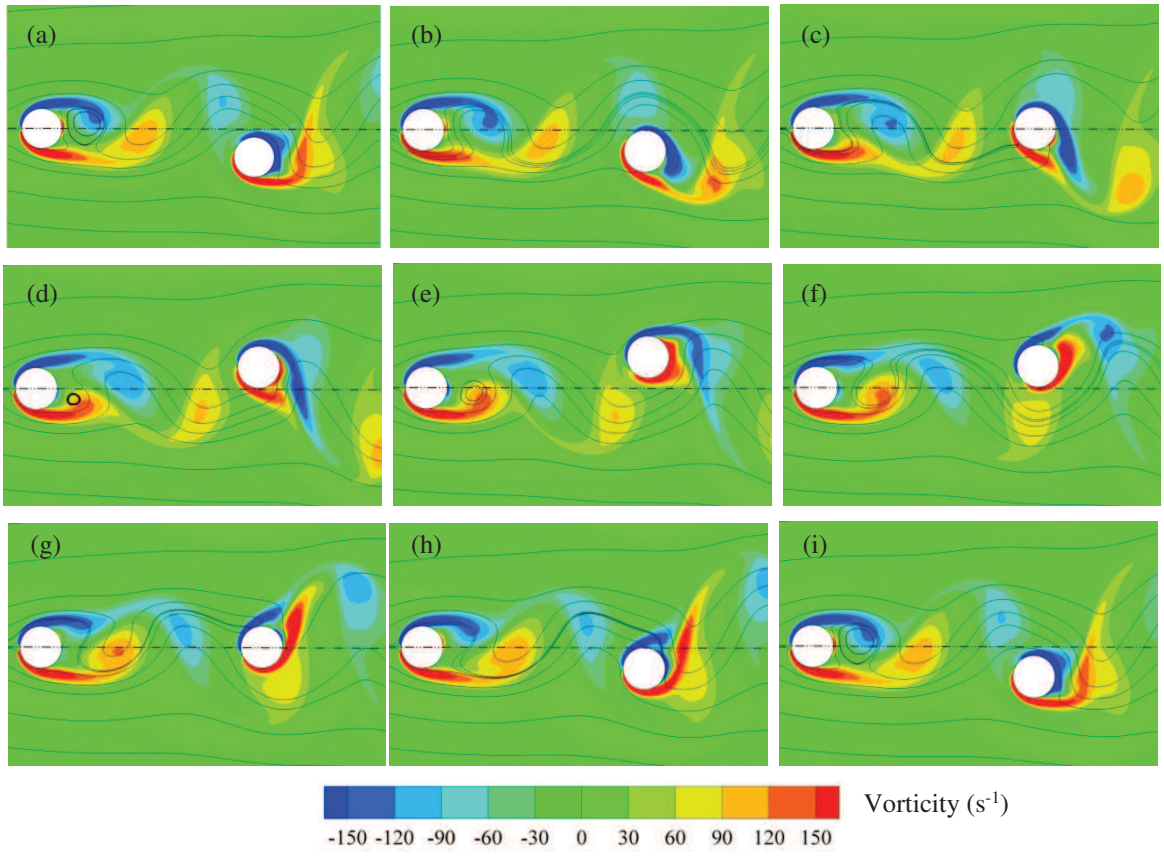


**Figure 10:** Vorticity and streamlines around cylinders for Re = 118 at nine instants (shown in the graph in Fig. 9) during one cycle

## 4 CONCLUSION

This paper presented a numerical analysis of a uniform flow over circular cylinders in tandem arrangement with center to center distance equal to 5.25$D$. Simulations were carried

out by using Ifeinco model which is based on the finite element method and employs the semi-implicit two-step Taylor-Galerkin method to discretize the Navier-Stokes equations and the Newmark method for the dynamic equation of the structure.

The root mean square of lift coefficient, the mean drag coefficient and the Strouhal number at Reynolds number ranging from 90 to 140 for both stationary cylinders were compared with those obtained for a single cylinder. Important differences were observed: the lift coefficients of the downstream cylinder in tandem arrangement were much higher than those of the single cylinder, whereas its drag coefficients were around half of the value; Strouhal numbers are about 10% lower.

Considering the downstream cylinder elastically mounted in transversal direction, the lock-in region was captured by Reynolds number from 115 to 120; this range was different from and shorter than the one for the single cylinder (102 to 113). The maximum vibration amplitude, which was 0.721*D*, was higher than the one for the single cylinder (0.422*D*). At Re = 120 (in the lock-in region), the drag coefficient and the lift coefficient showed abrupt variations; the latter was much more intense. Complex interference occurs between both cylinders since the downstream cylinder is immersed in the periodic wake of the upstream one.

## REFERENCES


[1] Igarashi, T. Characteristics of the flow around two circular cylinders arranged in tandem. *Bulletin of JSME* (1977) **24**(188):323-331.

[2] Zdravkovich, M.M. Review of flow interference between two circular cylinders in various arrangements. *ASME Journal of Fluids Engineering* (1977) **99**:618-633.

[3] Zdravkovich, M.M. The effects of interference between circular cylinders in cross flow. *Journal of Fluids and Structures* (1987) **1**:618-633.

[4] Sumner, D., Price, S.J. and Païdoussis, M.P. Flow-pattern identification for two-staggered circular cylinders in cross-flow. *Journal of Fluid Mechanics* (2000) **411**:263-303.

[5] Didier, E. Numerical simulation of low Reynolds number flows over two circular cylinders in tandem. *Conference on Modelling Fluid Flow*, Budapest, September 9-12, (2009) 347-354.

[6] Zdravkovich, M.M. Flow induced oscillations of two interfering circular cylinders. *Journal of Sound and Vibration* (1985) **101**(4):511-521.

[7] Brika, D. and Laneville, A. The flow interaction between a stationary cylinder and a downstream flexible cylinder. *Journal of Fluids and Structures* (1999) **13**:579-606.

[8] Assi, G.R.S., Meneghini, J.R., Aranha. J.A.P., Bearman, P.W. and Casaprima, E. Experimental investigation of flow-induced vibration interference between two circular cylinders. *Journal of Fluids and Structures* (2006) **22**: 819:827.

[9] Okajima, A., Yasui, A., Kiwata, T. and Kimura, S. Flow-induced treamwise oscillation of two circular cylinders in tandem arrangement. *International Journal of Heat and Fluid Flow* (2007) **28**:552-560.

[10] Huera-Huarte, F.J. and Gharib, M. Vortex- and wake-induced vibrations of a tandem arrangement of two flexible circular cylinders with far wake interference. *Journal of Fluids and Structures* (2011) **27**:824-828.

[11] Li, J., Chambarel, A., Donneaud, M. and Martin, R. Numerical study of laminar flow past one and two circular cylinders. *Computers & Fluids* (1991) **19**:155-170.

[12] Slaouti, A. and Stanby, P.K. Flow around two circular cylinders by the random-vortex method. *Journal of Fluids and Structures* (1992) **6**:641-670.
[13] Mittal, S., Kumar, V. and Raghuvanshi A. Unsteady incompressible flows past two cylinders in tandem and staggered arrangements. *International Journal for Numerical Methods in Fluids* (1997) **25**:1315-1344.
[14] Meneghini, J.R., Saltara, F., Siqueira, C.L. and Ferrari, J.A. Numerical simulation of flow interference between two circular cylinders in tandem and side by side arrangements. *Journal of Fluids and Structures* (2001) **15**:327-350.
[15] Sharman, B.. Lien, F.S., Davidson, L. And Norberg, C. Numerical predicitions of low Reynolds number flows over two tandem circular cylinders. *International Journal for Numerical Methods in Fluids* (2005) **47**:423-447.
[16] Carmo, B.S. Estudo numérico do escoamento ao redor de cilindros alinhados. Master Thesis, Escola Politécnica da Universidade de São Paulo (2005).
[17] Carmo, B.S. and Meneghini, J.R. Numerical investigation of the flow around two circular cylinders in tandem. *Journal of Fluids and Structures* (2006) **22**:979-988.
[18] Carmo, B.S., Sherwin, S.J., Bearman, P.W. and Willden, R.H.J. Flow-induced vibration of a circular cylinder subjected to wake intereference at low Reynolds number. *Journal of Fluids and Structures* (2011) **27**:503-522.
[19] Mittal, S. and Kumar, V. Flow-induced oscillations of two cylinders in tandem and staggered arrangements. *Journal of Fluids and Structures* (2001) **15:**717-736.
[20] Papaioannou, G.V., Yue, D.K.P., Triantafyllou, M.S. and Karniadakis, G.E. On the effect of spacing on the vortex-induced vibrations of two tandem cylinders. *Journal of Fluids and Structures* (2008) **24**:833-854.
[21] Teixeira, P.R.F. and Awruch, A.M. Numerical simulation of fluid-structure interaction using the finite element method. *Computers & Fluids* (2005) **34**:249–273.
[22] Teixeira, P.R.F. and Awruch, A.M. Three–dimensional simulation of high compressible flows using a multi-time-step integration technique with subcycles. *Applied Mathematical Modelling* (2001) **25**:613–627.
[23] Argyris, J., Doltsinis, J.St., Wuestenberg, H. and Pimenta, P.M. *Finite element solution of viscous flow problems*. Finite Elements in Fluids. Wiley, New York, Vol. 6, 89–114, (1985).
[24] Donea J., Giuliani, S., Laval and H., Quartapelle, L. Finite element solution of the unsteady Navier-Stokes equations by a fractional step method. *Computer Methods in Applied Mechanics and Engineering* (1982) **33**:53–73.
[25] Bathe, K.J. *Finite element procedures*. Prentice-Hall, (1996).
[26] Fredsϕe, J. and Sumer, B.M. *Hydrodynamics around cylindrical structures*. World Scientific Publishing Co. Pte. Ltd., Singapore, Vol. 12, (1997).
[27] Gonçalves, R.A., Teixeira P.R.F. and Didier, E. Numerical simulations of low Reynolds number flows past elastically mounted cylinder. *Thermal Engineering* (2012) **11**(1-2):61-67.